

Generalized Noise Analysis of Active Mixers by Simple Linear Periodic Time-Varying Circuit Model

Jongrit Lerdworatawee, Won Namgoong
 Department of Electrical Engineering
 University of Southern California

Abstract—A simple linear periodic time-varying circuit model is proposed to rigorously analyze the noise behavior in active mixers. Explicit formulas for thermal noise folding factor and flicker noise leakage are derived. Based upon our analysis, mixers operating at the OFF overlap mode are shown to provide better noise performance. The analysis is validated against simulations and measurements.

I. INTRODUCTION

As frequency translation devices, mixers are used to down convert the input radio frequency (RF) signal to the intermediate or dc frequency (IF) by the multiplication with a local oscillator (LO) signal. There exists two widely-used mixers: the active and passive one [1]. Using the switched differential pairs, the former commutates the signal current; whereas the latter commutates the signal voltage. Due to higher conversion gain, the active mixer can effectively suppress the noise contribution from the subsequent stages. For this reason, the active mixer is more attractive and commonly used at the front-end of various wireless receiver [2].

Mixer noise, particularly flicker noise in CMOS mixers, can significantly degrade the overall noise performance of the narrow-band receiving system like the direct conversion receiver (DCR). A simple physical model has been proposed for the mixer noise analysis as described in [3]. The switching pairs contribute flicker noise to the output through the direct and indirect mechanism. The former is by random modulation of the duty cycle of the output current whereas the latter is by charging and discharging of the tail capacitor. To reduce the flicker noise due to both mechanisms, the active mixer is suggested to operate in the OFF overlap mode, as is not commonly done in passive mixers [4][5].

To better understand the noise behavior under the OFF overlap condition, the noise analysis in [3] is more rigorously analyzed by modeling the mixer as a linear periodic time-varying (LPTV) system. This analysis is also a generalization of [6], which assumes that the mixers are memoryless devices and, as a result, is valid for low frequency only. In this paper, explicit formula for the mixer output noise statistic is derived. A comparison between the ON and OFF overlap mode is carried out in terms of thermal noise folding effect and the flicker noise leakage. The analysis is validated against simulation and measurement.

The paper is organized as follows. Section 2 presents the noise analysis, where thermal noise folding effect and the flicker noise leakages are derived. Simulation and measurement results are provided in Section 3. Conclusions are drawn in Section 4.

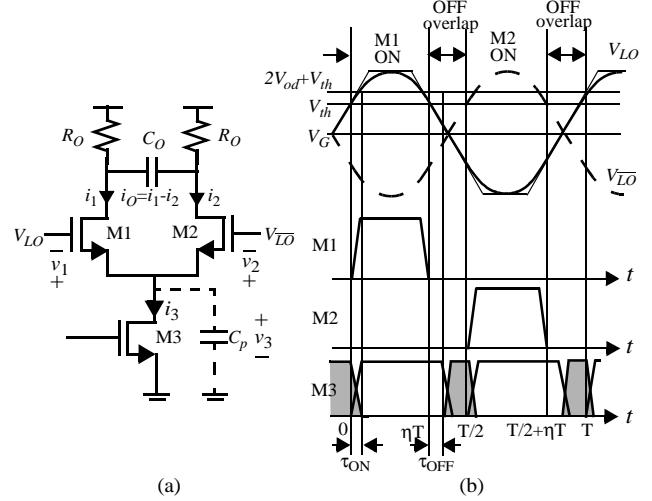


Fig. 1. single-balance active CMOS mixer

II. NOISE ANALYSIS

A. Large-Signal Modeling

Fig. 1(a) shows a single-balanced CMOS active mixer, which consists of an input transconductance device (M3), symmetric switched differential pairs (M1 and M2) and an output low-pass RC filter. The gate of M1 and M2 are biased by two anti-phase sinusoidal signals of period $T (=1/f_{LO})$, i.e., $V_{LO} = V_G + A_{LO} \sin \omega_{LO} t$ and $V_{\bar{LO}} = V_G - A_{LO} \sin \omega_{LO} t$, where V_G is the common voltage and A_{LO} is the amplitude. For the mixer to operate in the OFF overlap mode, V_G must be less than the device threshold voltage (V_{th}). Fig. 1(b) presents an example of V_{LO} (and $V_{\bar{LO}}$) where the OFF overlap occurs when both V_{LO} and $V_{\bar{LO}}$ are less than V_{th} . Away from the OFF overlap, M1 (or M2) is instantaneously in saturation; while M3 experiences a delay τ_{ON} . During the OFF overlap, M1 and M2 are OFF; whereas M3 remains in saturation region for τ_{OFF} before entering into the linear region.

To simplify the analysis, V_{LO} (and $V_{\bar{LO}}$) is linear piecewise approximated by a trapezoid function. With this approximation, V_{LO} (and $V_{\bar{LO}}$), the transconductance ($g_m(t)$) and drain conductance ($g_{ds}(t)$) are illustrated as shown in Fig. 1(b). In this Figure, the time interval when M1 (or M2) is ON is $[\eta T, T/2]$ and $[T/2 + \eta T, T]$. Here η is the duty cycle which can be determined by

$$\eta = \frac{1}{2} - \left(\frac{V_{th} - V_G}{\pi A_{LO}} \right) \quad (1)$$

where A_{LO} must be no less than $|V_{th} - V_G|$. For sufficiently high A_{LO} , the trapezoid function becomes a perfect square waveform with

duty cycle of η , which increases (or reduces) to 50% with increasing A_{LO} (see (1)) when the mixer operates in the OFF (or ON) overlap mode. As a result, τ_{ON} can be neglected and $\tau_{OFF} = C_p(V_{LOpeak} - V_{th} - 2V_{od})/I_{d3}$, where C_p is the total capacitor at the drain of M3 and assumed constant, V_{LOpeak} is the peak voltage of V_{LO} , V_{od} is the gate overdrive voltage and I_{d3} is the tail current.

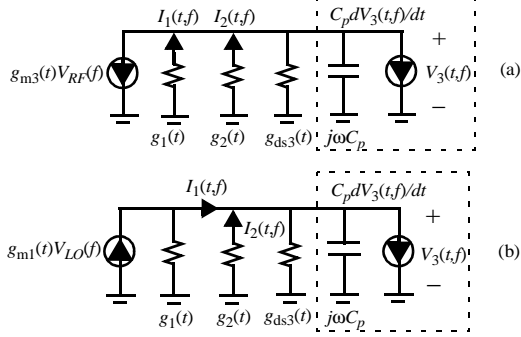


Fig. 2. LPTV circuit model

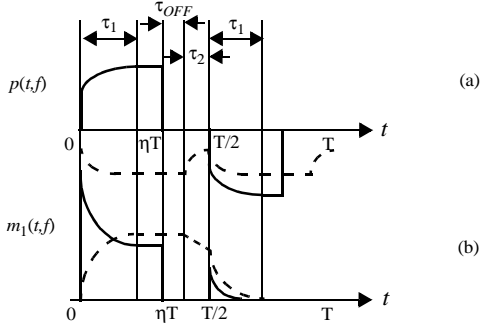


Fig. 3. $p(t,f)$ and $m_1(t,f)$.

B. Small-Signal LPTV Analysis

The systematic approach to analyze the mixer is to model it as a linear periodic time-varying (LPTV) system. Unlike the linear time-invariant (LTI) system, the transfer function varies as a function of time. To obtain the transfer function, we linearize a set of nonlinear equations describing the mixer behavior around a time-varying operating point and solve the resulting equations.

For example, consider an input signal $v_{RF}(t) (=V_{RF}(f)\exp(j\omega t))$ presented at the gate of M3 and a vector of the state variables $\mathbf{v}(t) (= [v_1(t), v_2(t), v_3(t)]^T)$ (where $v_i(t)$ for $i=1,2$ and 3 are shown in Fig. 1(a)), whose amplitude is periodic time-varying, i.e., $\mathbf{v}(t) = \mathbf{V}(t,f)\exp(j\omega t)$ and $\mathbf{V}(t,f) = \mathbf{V}(t+T,f)$. To obtain $\mathbf{V}(t,f)$, one solves for the differential algebraic equation (DAE) in frequency domain [7], i.e.,

$$\left[\mathbf{C}(t) \frac{\partial}{\partial t} + \mathbf{G}_{eff}(t,f) \right] \mathbf{V}(t,f) = \mathbf{b} g_{m3}(t) V_{RF}(f) \quad (2)$$

where $\mathbf{b} = [1 \ 0]^T$ is a vector mapping the input node to the output. In (2), the capacitive effect is included by $\mathbf{C}(t) \partial / \partial t$ and $\mathbf{G}_{eff}(t,f) = \mathbf{G}(t) + j\omega \mathbf{C}(t)$, where $\mathbf{C}(t)$ and $\mathbf{G}(t)$ are the time-varying capacitance and conductance matrices as given by

$$\mathbf{C}(t) = \begin{bmatrix} 0 & 0 & C_p \\ 0 & 0 & 0 \\ 0 & 0 & 0 \end{bmatrix} \quad \text{and} \quad \mathbf{G}(t) = \begin{bmatrix} g_1(t) & g_2(t) & g_{ds3}(t) \\ 1 & -1 & 0 \\ 1/2 & 1/2 & -1 \end{bmatrix} \quad (3)$$

where $g_1(t) = g_{m1}(t) + g_{ds1}(t)$ and $g_2(t) = g_{m2}(t) + g_{ds2}(t)$. To solve (2), the numerical technique such as the time-domain shooting method or the frequency-domain harmonic balance technique is traditionally used [7]. These numerical methods are however generally computationally expensive in practice and rarely provide useful insights.

Instead, an analytical approach based on the circuit analysis is employed. This approach is to map the DAE in (2) to the equivalent circuit model and solve for the time-varying frequency response. Fig. 2 shows the equivalent circuit models with given inputs at the gate of M3 and M1. In this model, the gate of M1 and M2 are considered grounded and the resulting $v_1(t)$, $v_2(t)$ and $v_3(t)$ are the same and their amplitudes are denoted by $V_3(t,f)$. To include the capacitive effect which is modeled by $\mathbf{G}_{eff}(t,f)$, the capacitive element is substituted by a parallel connected capacitor and a voltage controlled current source, as illustrated by the dashed line block in Fig. 2. It is worth noting that when the capacitive effect is neglected, i.e., $C_p \approx 0$, the resulting solution becomes the same as in [6].

Using the circuit model in Fig. 2, Fig. 3 shows the resulting transfer function $p(t,f) (= (I_1(t,f) - I_2(t,f)) / V_{RF}(f))$ and $m_1(t,f) (= (I_1(t,f) - I_2(t,f)) / V_{LO}(f))$ represented by the bold lines and $V_3(t,f)$ by the dashed line. The explicit formulae for $p(t,f)$ and $m_1(t,f)$ can given by

$$p(t,f) = \sum_{k=-\infty}^{\infty} (-1)^k g_{m3} F(f) w_{\eta} \left(t - k \frac{T}{2} \right) \left\{ 1 - [1 - (1 - \xi_1) \xi_2] \exp \left(-\frac{(t - kT/2)}{\tau_1} \right) \right\} \quad (4)$$

$$m_1(t,f) = \sum_{k=-\infty}^{\infty} g_{m1} \left\{ \left[\bar{F}(f) + F(f) \exp \left\{ -\frac{(t - kT)}{\tau_1} \right\} \right] w_{\eta}(t - kT) + F(f) (1 - \xi_1) \xi_2 \exp \left\{ -\frac{(t - (k + \eta)T)}{\tau_1} \right\} \right\} w_{\eta} \left(t - \left(k + \frac{1}{2} \right) T \right) \quad (5)$$

where

$$F(f) = \frac{g_{1,sat}}{g_{1,sat} + g_{ds3,sat} + j\omega C_p} \quad (6)$$

and $\bar{F}(f) = 1 - F(f)$. In (4)-(5), $\tau_1 (= C_p / (g_{1,sat} + g_{ds3,sat}))$ and $\tau_2 (= C_p / g_{ds3,lin})$ are respectively the time constants when M3 is in saturation and linear region; $\xi_1 = \exp\{-\eta T / \tau_1\}$, $\xi_2 = \exp\{-((1/2 - \eta)T - \tau_{OFF}) / \tau_2\}$ and $w_{\eta}(t) = u(t) - u(t - \eta T)$. From Fig. 3(b), note that a second pulse of $m_1(t,f)$ in the last half period of V_{LO} depends on τ_{OFF} during which $V_3(t,f)$ remains unchanged. The consequence will be discussed in greater detail shortly. Since M1 and M2 are assumed symmetric, the transfer function from the gate of M2 to the output can be determined by $m_2(t,f) = m_1(t - T/2, f)$.

C. Mixer Output Noise PSD

For noise analysis in the CMOS mixers, the input noise sources (generated in M1-M3) mainly consist of the flicker noise at low frequency and the thermal noise at high frequency. Assuming that a output low-pass filter has a 3dB bandwidth less than $1/T$, the output noise can be assumed to be a stationary process whose PSD is defined in terms of the average PSD [8]

$$S_{N_o}(f) = \sum_{n=-\infty}^{\infty} |p^{(n)}(f)|^2 S_{N_x}(f - nf_{LO}) \quad (7)$$

$$+ \sum_{n=-\infty}^{\infty} |m_1^{(n)}(f)|^2 (S_{N_1}(f - nf_{LO}) + S_{N_2}(f - nf_{LO}))$$

$$\approx 4kT \left[\left(\frac{\gamma}{g_{m3, sat}} \right) \underbrace{\sum_{n=-\infty}^{\infty} |p^{(n)}(f)|^2}_{\alpha(f)} + 2 \left(\frac{K}{WLC_{ox}f} \right) \underbrace{m_1^{(0)}(f)}_{\beta(f)} \right]$$

where S_{N_x} is the noise PSD generated in MX for X=1, 2 and 3; $p^{(n)}(f)$ and $m_1^{(n)}(f)$ are the nth order harmonic transfer functions of $p(t,f)$ and $m_1(t,f)$; γ and K are the thermal and flicker noise coefficient; $\alpha(f)$ and $\beta(f)$ are known as the thermal noise folding factor and flicker noise leakage.

With good device matching, $p(t,f) = p(t-T/2, f)$, $p(t,f)$ has only the odd-order harmonic transfer functions, i.e., for n is odd number,

$$p^{(n)}(f) = \frac{1}{T} \int_0^T p(t, f - nf_{LO}) e^{-jn\omega_{LO}t} dt \quad (8)$$

$$= p_n \cdot g_{m3} F(f - nf_{LO})$$

where

$$\Re\{p_n\} = \frac{(1 - \cos 2n\pi\eta)}{n\pi} \left\{ \frac{1 - \xi_1 \left(\cos 2n\pi\eta + \frac{f_T}{nf_{LO}} \sin 2n\pi\eta \right)}{n\pi \left[1 + \left(\frac{f_T}{nf_{LO}} \right)^2 \right]} - [1 - (1 - \xi_1)\xi_2] \right\} \quad (9)$$

$$\Im\{p_n\} = \frac{\sin 2n\pi\eta}{n\pi} \left\{ \frac{1 - \xi_1 \left(\cos 2n\pi\eta - \frac{nf_{LO}}{f_T} \sin 2n\pi\eta \right)}{n\pi \left[1 + \left(\frac{f_T}{nf_{LO}} \right)^2 \right]} - [1 - (1 - \xi_1)\xi_2] \right\} \quad (10)$$

where $f_T = 1/(2\pi\tau_1)$. (8) suggests that only the high frequency thermal noise generated in M3 is translated down to the output and the resulting noise floor is scaled by α . As $p^{(n)}(f)$ is centered at nf_{LO} and band-limited to f_T , α is much smaller than what is predicted under the conventional memoryless assumption.

On the other hand, $m_1(t,f)$ as shown in Fig. 3(b) turns out to be an impulse train, which has a non-zero DC term. This DC term is

the cause for leakage of the flicker noise from the switched differential pairs. By averaging $m_1(t,f)$ over a period of T ,

$$m_1^{(0)}(f) = \frac{1}{T} \int_0^T m_1(t, f) dt \quad (11)$$

$$= g_{m1} \left\{ \bar{F}(f)\eta + F(f) \underbrace{(\tau_1 f_{LO})(1 - \xi_1)[1 + \xi_2(1 - \xi_3)]}_{\delta} \right\}$$

where $\xi_3 = \exp\{-(1-\eta)T/\tau_1\}$. When $\eta=50\%$ and at near dc frequency, this flicker noise leakage has been predicted by means of the indirect mechanism as reported in [3]. Using the LPTV model in our analysis, the indirect mechanism can be better understood, which is applicable over a wider range of operations.

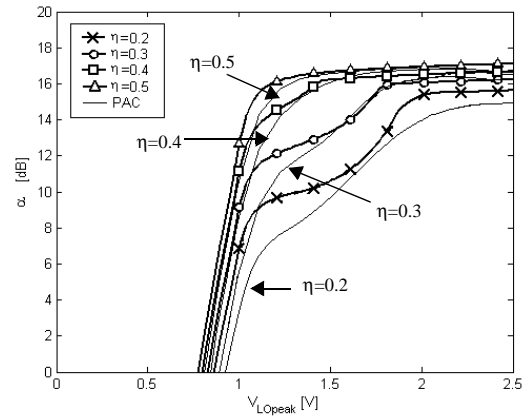


Fig. 4. simulated α

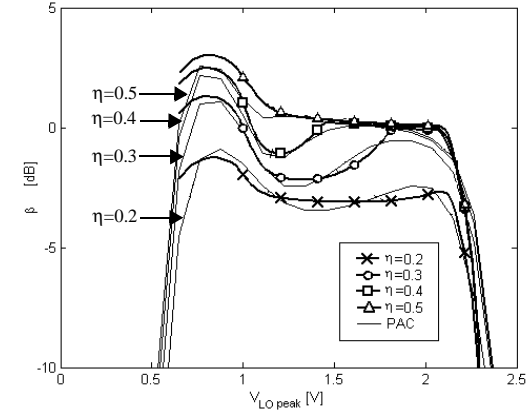


Fig. 5. simulated β

III. SIMULATION AND MEASUREMENT RESULTS

To validate our analysis, Fig. 4 and Fig. 5 show α and β using (10) and (11) (as illustrated by the bold solid line) against $V_{LO, peak}$, assuming $f_{LO}=1\text{GHz}$ and $f_{IF}=10\text{KHz}$. Using the standard $0.35\mu\text{m}$ CMOS technology, M1, M2 and M3 are sized with $200\mu\text{m}/0.35\mu\text{m}$ and the resulting g_m and g_{ds} are described using the non-quasi static short-channel model [9]. For comparison, the periodic steady state AC (PAC) analysis provided in Cadence SPECTRE-

RF package is used. The LO signals for both cases were given by the square waveforms with different η varying from 0.2 to 0.5 (as illustrated by the solid line).

The validity of our analysis is justified by the PAC simulation as shown in Fig. 4 and Fig. 5. The following important observations are made. First, unlike α , a peaking of β is observed with increasing $V_{LO,peak}$. This occurs because since β is proportional to the weighted sum of η and δ (see (11)), the value of β shifts from η to δ as $V_{LO,peak}$ increases. Since η is greater than δ , decreasing β is expected. Second, by further increasing $V_{LO,peak}$, both α and β with low η values will merge to α and β with $\eta=50\%$. This is because, for higher $V_{LO,peak}$, τ_{OFF} becomes larger and requires a longer time for M3 to return back from saturation to linear region during the OFF overlap time interval. Consequently, the effect of η on $p(t,f)$ and $m_1(t,f)$ is reduced. Finally, M1 (or M2) is pushed into the linear mode after $V_{LO,peak}$ is greater than 2V. Since this results in decreasing g_{m1} but increasing g_{ds1} , β is effectively reduced without significantly degrading α . A non-decreasing α is desired as it related to the conversion gain.

The advantage of allowing for the active mixer to operate in the OFF overlap mode becomes clear as β is reduced by 5dB when $\eta=20\%$ and $V_{LO,peak}$ is greater than 1.3V (see Fig. 5). This condition can be accomplished by employing a sinusoidal LO signal according to (1). To validate our analysis, Fig. 6 shows the measured flicker noise PSD between 10KHz and 500KHz at $f_{LO}=1\text{GHz}$. In this Figure, three operating conditions for the switched differential pairs are assumed: constant biasing at $V_{LO}=V_G=2\text{V}$; the ON overlap mode when $V_G=1\text{V}$ and $A_{LO}=1\text{V}$; and the OFF overlap mode when $V_G=0\text{V}$ and $A_{LO}=2\text{V}$. The measured noise spectrums are illustrated by the solid line while the estimations using (7) are by the dotted lines. A close agreement between our analysis and measurement are observed. In addition, a 5dB difference in noise spectrum between the ON and OFF overlap is verified.

IV. CONCLUSIONS

This paper presents a simple analytical LPTV circuit model to analyze the noise behavior of the active mixer. Using this model, the thermal noise folding and flicker noise leakage are derived. The advantage of having the mixer operating at the OFF overlap is observed and justified by simulations and measurements.

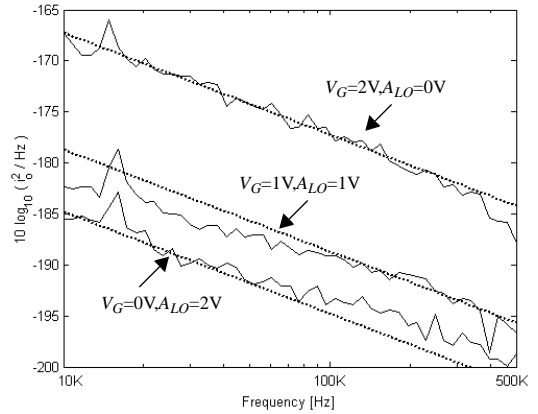


Fig. 6. measured flicker noise PSD

REFERENCES

- [1] T. H. Lee, *The Design of Radio-Frequency Integrated Circuits*, Cambridge, 1998.
- [2] A. R. Shahani, D. K. Shaeffer and T. H. Lee, "A 12-mW wide dynamic range CMOS front-end for a portable GPS receiver," *IEEE J. Solid-State Circuits*, vol. 32, pp. 2061 - 2070, Dec. 1997
- [3] H. Darabi and A. A. Abidi, "Noise in RF-CMOS mixers: A simple physical model," *IEEE J. Solid-State Circuits*, vol. 35, pp. 15-25, Jan.2000.
- [4] D. Ham and A. Hajimiri, "Complete noise analysis for CMOS switching mixers via stochastic differential equations," *Proceeding of CICC*, pp. 439-442, 2000.
- [5] S. Chehrazi, R. Bagheri and A. A. Abidi, "Noise in passive FET mixers: a simple physical model," *Proceeding of CICC*, pp. 375-378, 2004.
- [6] M. T. Terrovitis and R. G. Meyer, "Noise in current-commutating CMOS mixers," *IEEE J. Solid-State Circuits*, vol. 34, pp. 772-783, June 1999.
- [7] J. Roychowdhury, "Reduced-order modeling of time-varying systems," *IEEE Trans. Circuits Syst. II*, vol. 46, pp. 1273-1288, Oct. 1999.
- [8] W. A. Garner, *Introduction to Random Processes with Applications to Signals and Systems*, 2nd ed., McGraw-Hill, 1989.
- [9] Y. Tsidividis, *Operation and Modeling of the MOS Transistor*, 2nd ed., McGraw-Hill, 1999.